

Heavy Quark Decays^a

PERSIS S. DRELL

*Cornell University, Newman Laboratory
Ithaca, NY 14853-5001***1 Introduction**

The field of heavy quark decays was born in 1976 with the discovery of the D meson at SPEAR¹, and has blossomed ever since. By 1981, the weak decays of heavy quarks merited their own byline at Lepton–Photon in Bonn² and that tradition has continued to the present day.

The new results on heavy quark decays submitted to this year’s Lepton–Photon Conference naturally fell into two categories around which this review is organized. These are heavy quark decays at tree level and heavy quark decays beyond tree level.

Heavy quark decays at tree level have been studied since 1976, and this is indeed a very mature field. These analyses have two goals. The first is the study of decay dynamics and the effects of the strong interactions on the underlying weak decay. The second goal is to measure the magnitudes of the elements of the CKM matrix, $|V_{ub}|$ and $|V_{cb}|$, that represent quark flavor mixing³, thereby serving to define the Standard Model. Rather than summarizing the status of the tree level decays which has been done recently in several excellent reviews^{4,5}, I will focus here on several new analyses that are probing the details of b heavy quark decays at tree level and testing our understanding of them. I will also review charm decays that are aiding us in this effort.

The second category of heavy quark studies, heavy quark decays beyond tree level, represents a new and emerging (anything but mature) field. Enormous data sets from CLEO and LEP are allowing b quark rare decays to be seen and measured for the first time, and there are many new results this year. The goals for these studies are either to uncover physics beyond the Standard Model or to probe the phases of the elements of the CKM matrix.

2 Heavy Quarks at Tree Level*2.1 Semileptonic B to Charm Decays and $|V_{cb}|$*

I will start my discussion of tree level heavy quark decays with semileptonic decays of the bottom quark as illustrated in figure 1. Semileptonic decays are among the most extensively studied of all heavy quark decays. This is due to their theoretical simplicity: the

^aInvited Talk at the XVIII International Symposium on Lepton-Photon Interactions

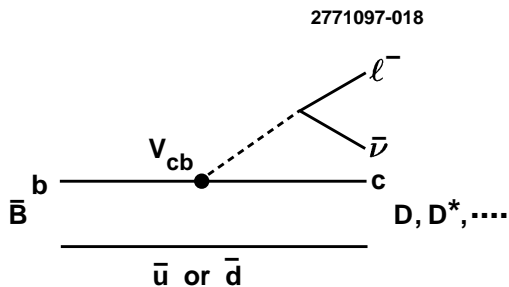


Figure 1: Diagram illustrating the semileptonic decay of a \bar{B} meson to a charm meson.

Table 1: Average inclusive and exclusive semileptonic branching ratios.

| Decay channel | World average branching ratio |
|--|-------------------------------|
| $\mathcal{B}(\bar{B} \rightarrow D\ell^-\bar{\nu})$ | 0.0195 ± 0.0027 |
| $\mathcal{B}(\bar{B} \rightarrow D^*\ell^-\bar{\nu})$ | 0.0505 ± 0.0025 |
| $\mathcal{B}(\bar{B} \rightarrow D^{(*)}\pi X\ell^-\bar{\nu})$ | 0.023 ± 0.0044 |
| $\mathcal{B}(\bar{B} \rightarrow X_u\ell^-\bar{\nu})$ | 0.0015 ± 0.001 |
| $\Sigma\mathcal{B}_i$ | 0.0945 ± 0.0058 |
| $\mathcal{B}(b \rightarrow q\ell^-\bar{\nu})^{\Upsilon(4S)}$ | 0.1018 ± 0.0040 |
| $\mathcal{B}(b \rightarrow q\ell^-\bar{\nu})^Z$ | 0.1095 ± 0.0032 |

matrix element can be written as a product of a leptonic current which is exactly known, and a hadronic current which can be parameterized in terms of form factors. Strong interactions are quite important in these decays, but they are sufficiently simple to allow detailed theoretical predictions that can be tested experimentally. These decays are experimentally accessible with relatively large branching ratios and clean signatures.

Exclusive and Inclusive B Semileptonic Branching Ratios

In table 1, I give updates on the average inclusive semileptonic B branching fractions as well as updates on the dominant exclusive semileptonic branching fractions. These branching fractions have changed very little in the last year. Figures 2 and 3 summarize the current experimental measurements from which the world averages are built.

The most basic check of our understanding of semileptonic B decays is to see that the sum of the exclusive modes is consistent with the inclusive rate. Do we understand all of the pieces of the semileptonic rate? The dominant semileptonic modes are reasonably well

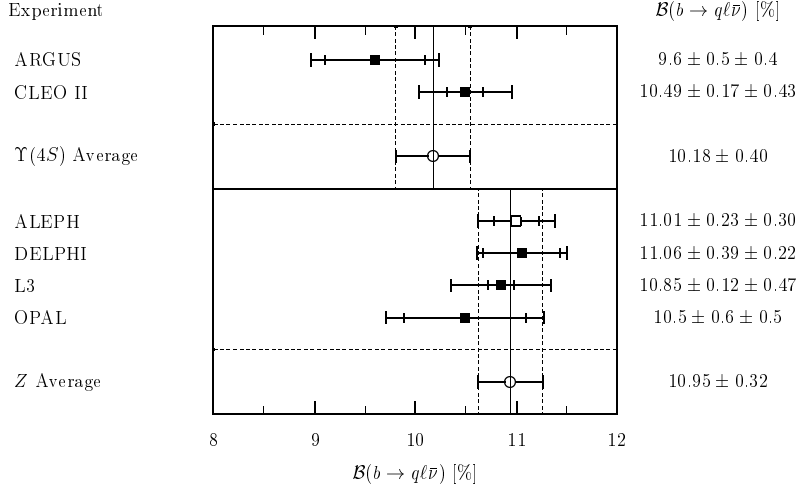


Figure 2: Summary of the measurements of the inclusive semileptonic branching ratio $\mathcal{B}(b \rightarrow q\ell\bar{\nu})$ from the $\Upsilon(4S)$ ⁶ and the Z ⁷.

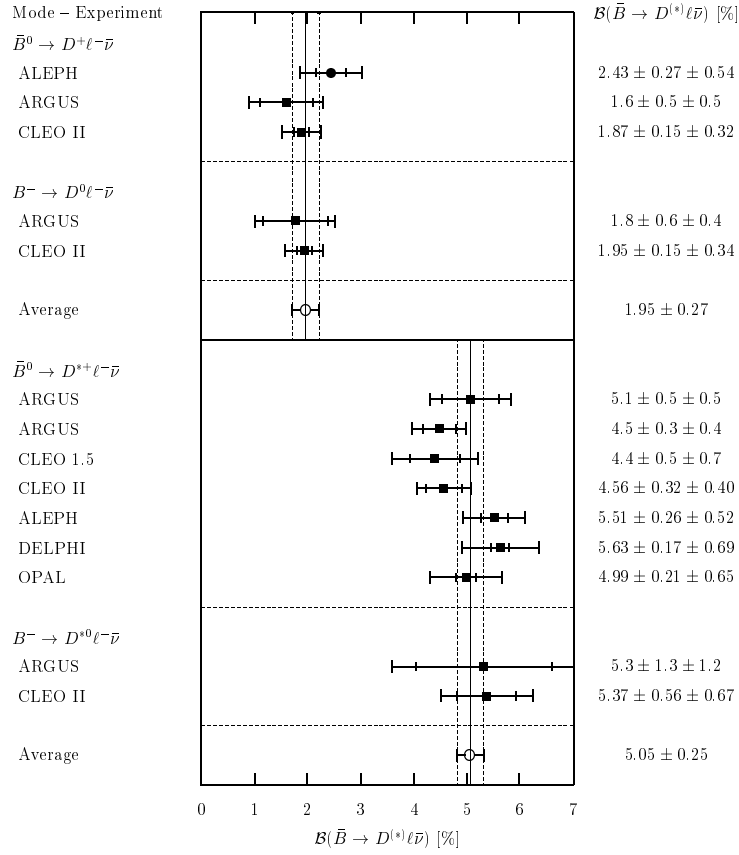


Figure 3: Summary of measurements of $\mathcal{B}(\bar{B} \rightarrow D\ell\bar{\nu})$ ⁸ and $\mathcal{B}(\bar{B} \rightarrow D^*\ell\bar{\nu})$ ^{9,10}. In the values listed, the branching ratios are updated to $\mathcal{B}(D^0 \rightarrow K^-\pi^+) = 0.0388 \pm 0.0010$ and $\mathcal{B}(D^+ \rightarrow K^-\pi^+\pi^+) = 0.088 \pm 0.006$

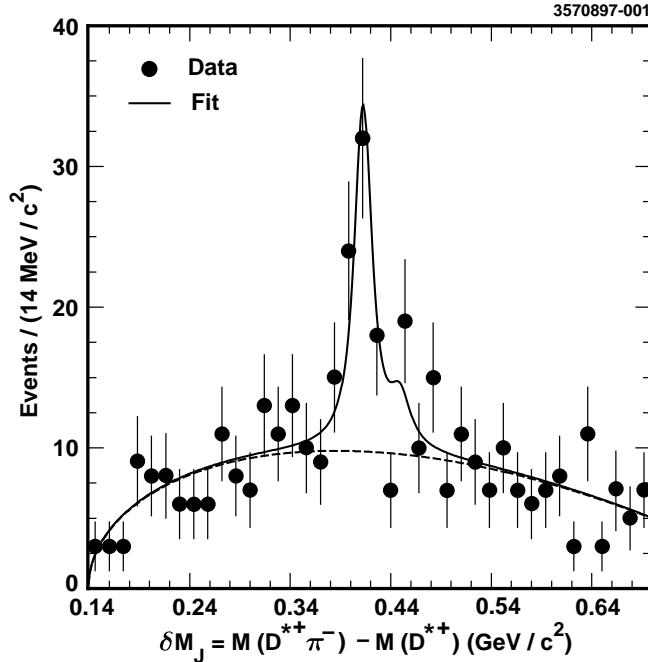


Figure 4: Observation of semileptonic B decay to a P wave charm meson by the CLEO detector. The mass difference $M(D^{*+}\pi^-) - M(D^{*+})$ is shown with a clear enhancement at the D_1 mass.

known; however they only account for 70 percent of the total semileptonic rate. The remaining 30 percent of the semileptonic rate is semileptonic decay to P wave and higher angular momentum charm states, to radially excited charm states, or to non-resonant $D^{(*)}\pi\ell^{-}\bar{\nu}$ states. The ALEPH collaboration has used a topological study to estimate the contribution to the semileptonic rate from states other than $D\ell^{-}\bar{\nu}$ and $D^*\ell^{-}\bar{\nu}$ ¹¹.

From table 1, we see that at the $1 - 2\sigma$ level, it appears that exclusives saturate the inclusions. However, of the 30% of the semileptonic rate that is not to $D\ell^{-}\bar{\nu}$ and $D^*\ell^{-}\bar{\nu}$, only one of the decays has been exclusively observed. Figure 4 shows the new CLEO result for $\bar{B} \rightarrow D_1\ell^{-}\bar{\nu}$ ¹² and figure 5 summarizes the ALEPH and CLEO measurements of $\bar{B} \rightarrow D_1\ell^{-}\bar{\nu}$. Both experiments also put upper limits on the amount of D_2^* production in semileptonic B decays at the 1% level. It is puzzling that the D_1 and D_2^* can account for so little of the total semileptonic rate, and detailed understanding of the decays other than $D\ell\bar{\nu}$ and $D^*\ell^{-}\bar{\nu}$ is absent.

HQET

Our understanding of how to interpret semileptonic heavy quark decays has evolved enormously with the development of heavy quark effective theory (HQET) ¹³. This allows us to extract CKM matrix elements from exclusive semileptonic B decays such as $\bar{B} \rightarrow D^*\ell^{-}\bar{\nu}$ with much greater confidence.

The central insight of HQET is to notice that a B meson or a charm meson (a light

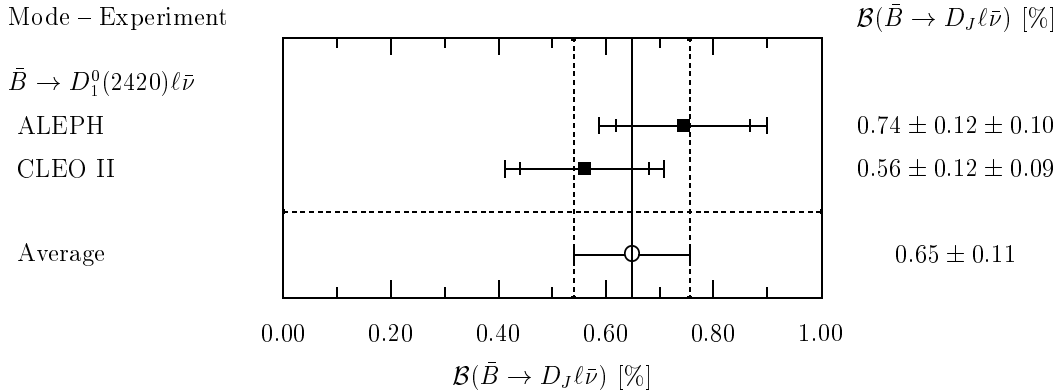


Figure 5: Summary of the CLEO¹² and ALEPH¹¹ measurements of $\mathcal{B}(\bar{B} \rightarrow D_1 \ell^- \bar{\nu})$.

quark bound to a very heavy quark) looks a lot like the hydrogen atom (a light electron bound to a heavy proton). If we recall that the e^- wave function in hydrogen looks just like the e^- wave function in deuterium up to hyperfine splittings, we expect that the light quark part of the B meson wave function should look just like the light quark part of the D meson wave function, up to hyperfine splittings of order Λ_{QCD}/M_Q , where M_Q is the mass of the heavy quark in the meson.

One consequence of this observation is that the rate for heavy meson to heavy meson semileptonic decays can be factorized into a heavy quark part which is calculable and a light quark overlap integral. This light quark overlap integral is not calculable from first principles but it is universal. It is the same for all heavy meson to heavy meson decays involving a pseudoscalar or vector meson (up to hyperfine effects). All three form factors needed to describe the hadronic current in $\bar{B} \rightarrow D^* \ell^- \bar{\nu}$ decay and the one form factor needed to describe $\bar{B} \rightarrow D \ell^- \bar{\nu}$ decay can be written as known quantities times one unknown function, $\xi(v \cdot v')$, where v and v' are the four velocities of the incoming and outgoing mesons respectively.

Extraction of $|V_{cb}|$

A standard method for extracting $|V_{cb}|$ in the past five years has been to use exclusive $\bar{B} \rightarrow D^* \ell^- \bar{\nu}$ decays and to take advantage of HQET. What makes HQET attractive in analyzing these decays is that at zero recoil, when the initial and final state mesons are at rest, the unknown function $\xi(v \cdot v')$ describing the overlap of the initial and final light quark wave functions is absolutely normalized. This absolute normalization is a result of the fact that in the zero recoil configuration, the light quark does not know or care that a heavy c quark has replaced a heavy b quark in the decay. The overlap is perfect. In the limit of infinitely heavy quarks, at this magic kinematic point, $|V_{cb}|$ can be measured independent of any unknown form factor. Effectively one trades statistics in data to measure $|V_{cb}|$ in a region of phase space where the form factor is well known.

In practice, the LEP experiments, ARGUS and CLEO have extracted $|V_{cb}|$ from $\bar{B} \rightarrow D^* \ell^- \bar{\nu}$ by measuring the differential decay rate as a function of $w = v \cdot v' = (m^2 + M^2 -$

$q^2)/(2mM)$, where M and m are the masses of the initial and final state mesons respectively¹⁴. In the limit of infinitely heavy quarks, the decay rate at zero recoil or $w = 1$ (corresponding to the maximum value of q^2 for the decay), where the light quark overlap integral or form factor is identically one, yields $|V_{cb}|$.

The differential decay rate can be expressed as:

$$\frac{d\Gamma}{dw} = \frac{G_F^2}{48\pi^3} \kappa(m_B, m_D, w) |V_{cb}|^2 \mathcal{F}^2(w) \quad (1)$$

where $\mathcal{F}(w) = \eta_A \hat{\xi}(w)$, and κ is a known function. In the limit of infinitely heavy quark masses, $\hat{\xi}(w)$ reduces to $\xi(w)$. η_A is a correction to the differential decay rate that can be calculated in perturbative QCD¹⁵.

There are several subtleties which must be kept in mind in this procedure. The experiments are now sufficiently precise that these corrections are important.

1. In the real world, q^2 or w is not reconstructed exactly. There is experimental smearing between the true value and reconstructed value. An unbinned maximum likelihood fit to the entire w distribution must be done to properly account for the smearing. Most experiments now use such a procedure.
2. Also in the real world, the c and b quark masses are not infinitely heavy, and the heavy quark symmetry limit is only the first term in an expansion in $1/M_Q$. The extrapolation to zero recoil gives the form factor at zero recoil, $\mathcal{F}(1)$, times $|V_{cb}|$. In the limit of infinite quark mass, $\mathcal{F}(1) = 1$. For finite mass quarks the corrections are substantial with significant errors^{16,17}:

$$\mathcal{F}(1)_{D^* \ell \nu} = 0.91 \pm 0.03 \quad (2)$$

$$\mathcal{F}(1)_{D \ell \nu} = 0.98 \pm 0.07 \quad (3)$$

3. The shape of the form factor distribution, $\mathcal{F}(w)$ is not known. This is important since the differential decay rate actually vanishes at zero recoil (since there is no phase space there). Experimentally, the decay rate is measured as a function of w and extrapolated to zero recoil using the form of a Taylor expansion for the form factor

$$\mathcal{F}(w) = \mathcal{F}(1) \left[1 - \hat{\rho}^2 (w - 1) + \hat{c} (w - 1)^2 + \dots \right] \quad (4)$$

Experiments are not yet sensitive to the quadratic term in the expansion and typically quote values of $|V_{cb}|$ from a linear fit. In the fits, the intercept and slope are highly correlated and a small correction to $|V_{cb}|$ of order 1×10^{-3} must be applied to compensate for the lack of curvature in the fit.

I follow the procedure outlined by Gibbons at Warsaw⁵ to extract a world average value for $|V_{cb}|$ from exclusive semileptonic B decays¹⁸. The experimental values for the intercept and the slope in these fits¹⁰, summarized in table 2 and figure 6, are combined with careful attention to the correlated errors yielding the values in table 3.

Table 2: The experimental values of $\mathcal{F}(1)|V_{cb}|$ and the slope, $\hat{\rho}^2$, of the form factor as extracted from exclusive semileptonic B decays¹⁰. $\tau_{B^0} = (1.55 \pm 0.04) \times 10^{-12}$ and $\tau_{-}/\tau_0 = 1.06 \pm 0.04$ ¹⁹ are used in converting the branching fractions into rates.

| Mode | Experiment | $\mathcal{F}(1) V_{cb} $ | $\hat{\rho}^2$ |
|--|------------|----------------------------------|-----------------------------|
| $\bar{B} \rightarrow D^* \ell^- \bar{\nu}$ | ALEPH | $0.03205 \pm 0.0018 \pm 0.0019$ | $0.31 \pm 0.17 \pm 0.08$ |
| | DELPHI | $0.0369 \pm 0.00209 \pm 0.00217$ | $0.782 \pm 0.187 \pm 0.036$ |
| | OPAL | $0.0326 \pm 0.0017 \pm 0.0022$ | $0.42 \pm 0.17 \pm 0.052$ |
| | CLEO | $0.03516 \pm 0.0019 \pm 0.00184$ | $0.84 \pm 0.12 \pm 0.08$ |
| | ARGUS | $0.0392 \pm 0.0039 \pm 0.0028$ | $1.17 \pm 0.24 \pm 0.06$ |
| $\bar{B} \rightarrow D \ell^- \bar{\nu}$ | ALEPH | $0.0282 \pm 0.0068 \pm 0.0065$ | $-0.05 \pm 0.53 \pm 0.38$ |
| | CLEO | $0.0342 \pm 0.0044 \pm 0.0049$ | $0.61 \pm 0.21 \pm 0.13$ |

Table 3: The world average values of $|V_{cb}|$ and the slope, $\hat{\rho}^2$, of the form factor $\mathcal{F}(1)$ as extracted from exclusive semileptonic B decays. $\tau_{B^0} = (1.55 \pm 0.04) \times 10^{-12}$ and $\tau_{-}/\tau_0 = 1.06 \pm 0.04$ ¹⁹ are used in converting the branching fractions into rates.

| Mode | $ V_{cb} $ | $\hat{\rho}^2$ |
|--|---------------------|-----------------|
| $\bar{B} \rightarrow D^* \ell^- \bar{\nu}$ | 0.0387 ± 0.0031 | 0.71 ± 0.11 |
| $\bar{B} \rightarrow D \ell^- \bar{\nu}$ | 0.0394 ± 0.0050 | 0.66 ± 0.19 |

Inclusive semileptonic decays are also used to extract $|V_{cb}|$. The dominant uncertainties in this procedure have traditionally been theoretical with typically ten percent errors assigned to the calculation of the rate, resulting in five percent errors on $|V_{cb}|$.

A series of theoretical papers have taken the formalism of HQET in combination with the techniques of the operator product expansion and shown that the inclusive $b \rightarrow c \ell^- \bar{\nu}$ rate is the leading term in a well-defined double expansion in α_s and Λ_{QCD}/M_Q , where the coefficients of the expansion involve matrix elements that reflect non perturbative effects²⁰. By experimentally measuring the moments of either the inclusive lepton spectrum or the hadronic mass spectrum squared in $b \rightarrow c \ell^- \bar{\nu}$ decays, these unknown matrix elements can be experimentally determined and then used, in combination with the measured inclusive semileptonic rate, to extract $|V_{cb}|$. I believe this offers real hope in improving the theoretical uncertainty on the extraction of $|V_{cb}|$ from the inclusive semileptonic rate, and experimental attempts to apply this formalism to data are in progress.

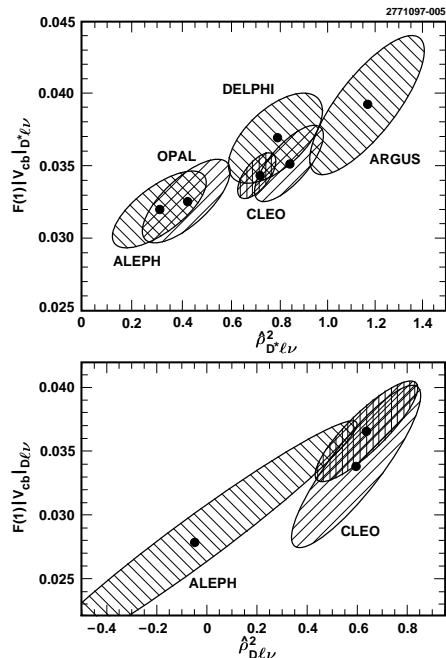


Figure 6: One standard deviation error ellipses for $\mathcal{F}(1)|V_{cb}|$ versus the form factor slope $\hat{\rho}^2$. The black cross-hatched ellipse is the world average. The upper plot is for the decay $\bar{B} \rightarrow D^* \ell^- \bar{\nu}$ and the lower plot is for the decay $\bar{B} \rightarrow D \ell^- \bar{\nu}$.

Figure 7 gives the world average values of $|V_{cb}|$ extracted using both inclusive and exclusive techniques. The excellent agreement between a wide variety of methods for extracting $|V_{cb}|$ is quite encouraging; however, given the broad range of estimates for the theoretical uncertainties and the primitive status of many of the experimental checks of theoretical inputs, I advise against averaging the results.

Checks of HQET

It is extremely important that we experimentally check the predictions of HQET. Several approaches to this have been used so far, although they are not yet precise enough to be considered true tests.

HQET predicts simple relations between the three form factors, A_1, A_2 and V that are needed to describe the hadronic current in $\bar{B} \rightarrow D^* \ell^- \bar{\nu}$ decays. These are usually expressed in terms of the form factor ratios, $R_1(w)$ and $R_2(w)$. By studying the full correlated angular distribution for these decays, CLEO has shown consistency between experimental data²¹ and the predictions of heavy quark symmetry^{22,23,24} as summarized in table 4. (Note: the interested reader can find the full expressions for the decay rate in terms of the form factors in a variety of excellent references. I particularly recommend Richman⁴ and Richman and Burchat²⁵.)

A second approach to checking HQET is to compare the slope of the form factor distribution, $\mathcal{F}(w)$, extracted from $\bar{B} \rightarrow D \ell^- \bar{\nu}$ and $\bar{B} \rightarrow D^* \ell^- \bar{\nu}$ decays. These slopes, which are

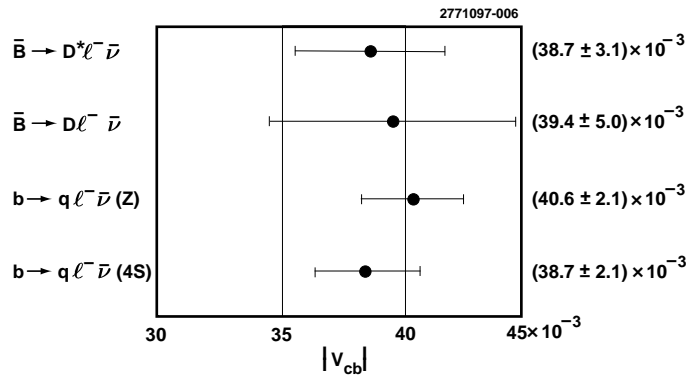


Figure 7: The world average values of $|V_{cb}|$ from a variety of techniques. The exclusive averages are described in this paper. The inclusive averages have not changed in the past year⁵.

Table 4: Form factor ratios in $\bar{B} \rightarrow D^* \ell^- \bar{\nu}$ decays as measured by CLEO.

| | $R_1(w = 1)$ | $R_2(w = 1)$ |
|---------------------------------|--------------------------|--------------------------|
| CLEO II ²¹ | $1.24 \pm 0.26 \pm 0.12$ | $0.72 \pm 0.18 \pm 0.07$ |
| Neubert ²² | 1.3 ± 0.1 | 0.8 ± 0.2 |
| Close and Wambach ²³ | 1.15 | 0.91 |
| ISGW2 ²⁴ | 1.27 | 1.01 |

given in table 3, should agree in the heavy quark limit, although finite mass corrections will be different for the two modes. The overall agreement between the slopes of $\mathcal{F}(w)$ for $\bar{B} \rightarrow D \ell^- \bar{\nu}$ and $\bar{B} \rightarrow D^* \ell^- \bar{\nu}$ is encouraging although the errors are large.

Yet another check is to compare $\hat{\rho}^2$, the slope of $\mathcal{F}(w)$ extracted from the $d\Gamma/dw$ distribution and given in table 3, with the form factor slope, $\rho_{A_1}^2 = 0.91 \pm 0.016$ that is extracted from fits to the full differential distribution²¹ for $\bar{B} \rightarrow D^* \ell^- \bar{\nu}$ decay. The slope of $\mathcal{F}(w)$ has a complicated dependence on all three hadronic form factors involved in the decay: $\hat{\rho}^2 = \rho_{A_1}^2 - f(R_1, R_2)$. Model dependent calculations¹⁷ suggest the relation $\hat{\rho}^2 \approx \rho_{A_1}^2 - 0.2$. The data are consistent with this prediction within large errors.

Finally, we can attempt to use the same machinery developed for $\bar{B} \rightarrow D^{(*)} \ell^- \bar{\nu}$ decays on $D \rightarrow \bar{K}^{(*)} \ell^+ \nu$ decays. The CKM matrix element for these charm semileptonic decays is known so that the form factor can be measured directly. Very clean signals are obtained in the charm hadroproduction fixed target experiment E791 taking full advantage of their

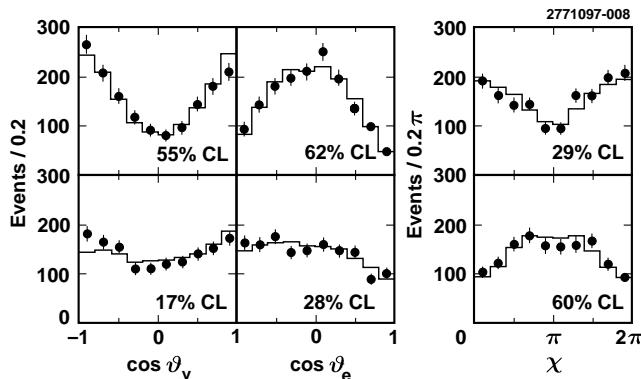


Figure 8: The kinematic distributions in $D \rightarrow \bar{K}^* \ell^+ \nu$ decay that are fit in the E791 analysis. The top row of plots is for the q^2 range: $q^2/q_{max}^2 \leq 0.5$ and the bottom row of plots is for $q^2/q_{max}^2 > 0.5$. The points are data and the histogram is the result of the fit.

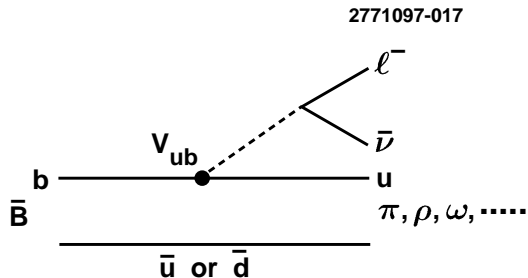


Figure 9: Diagram illustrating the semileptonic decays of a B meson to charmless final states.

23 planes of high resolution silicon strips to select separated charm vertices²⁶. They reconstruct 3000 $D \rightarrow \bar{K}^* \ell^+ \nu$ decays with very little background and then extract the form factors by doing a 4 dimensional fit to the kinematic variables describing the decay. Figure 8 shows the kinematic distributions that are fit in the E791 analysis. Again, the interested reader is referred to several excellent papers^{4,25} for the full expressions for the decay rate in terms of the form factors. While the s quark does not probably classify as heavy and so Λ/M_Q corrections will be large, the new results from E791 show quite good agreement with recent lattice calculations of the form factors as summarized in table 5.

I conclude that while we cannot claim yet that HQET has been experimentally verified by testing the $1/M_Q$ corrections to it, the exclusive semileptonic decays of bottom to charm are reasonably well understood experimentally and theoretically at this point.

2.2 Semileptonic Charmless B Decays and $|V_{ub}|$

Semileptonic B decays to charmless final states are used to measure $|V_{ub}|$. The basic process is illustrated in figure 9 and is the same as for semileptonic $b \rightarrow c \ell^+ \bar{\nu}$ decays except now the b quark turns into a u quark with coupling strength $|V_{ub}|$.

Table 5: Form factor ratios in $D \rightarrow \bar{K}^* \ell^+ \nu$ decays, as measured by E791, compared with various calculations.

| | $A_1(0)$ | $A_2(0)$ | $V(0)$ |
|---------------------|------------------------|------------------------|------------------------|
| E791 ²⁶ | 0.58 ± 0.03 | 0.41 ± 0.06 | 1.06 ± 0.09 |
| APE ²⁷ | 0.67 ± 0.11 | 0.49 ± 0.34 | 1.08 ± 0.22 |
| Wupp ²⁸ | 0.64 ± 0.06 | 0.61 ± 0.41 | 1.17 ± 0.38 |
| UKQCD ²⁹ | $0.70^{+0.07}_{-0.10}$ | $0.66^{+0.10}_{-0.15}$ | $1.01^{+0.30}_{-0.13}$ |
| ELC ³⁰ | 0.64 ± 0.16 | 0.41 ± 0.28 | 0.86 ± 0.24 |
| | $A_1(q_{max}^2)$ | $A_2(q_{max}^2)$ | $V(q_{max}^2)$ |
| E791 ²⁶ | 0.68 ± 0.04 | 0.48 ± 0.08 | 1.35 ± 0.12 |
| ISGW2 ²⁴ | 0.70 | 0.94 | 1.52 |

Exclusive and Inclusive Charmless B Semileptonic Branching Ratios

To date, inclusive searches for $b \rightarrow u \ell^- \bar{\nu}$ decays have been done at the $\Upsilon(4S)$ where B mesons are produced at rest ³¹. These analyses have looked at the endpoint of the single lepton spectrum for leptons from B decay that are kinematically incompatible with coming from the decay of a B meson to a charm meson. The b quark will preferentially turn into a c quark when it weakly decays, but c quarks are heavy. The lightest mass particle containing a charm quark is a D meson which has a mass of 1.8 GeV. In charmless decays, the final state hadronic mass can be as light as a pion mass. The difference in the final state hadronic mass is reflected in the momentum of leptons from the decaying B ; for a B meson at rest, the endpoint spectrum for leptons in charmless semileptonic decays extends about 300 MeV past the endpoint spectrum for semileptonic decays to charm. From the lepton excess in the endpoint region, one uses a model to extrapolate the full spectrum and extract:

$$|V_{ub}| = (3.1 \pm 0.8) \times 10^{-3} \quad (5)$$

The model uncertainty dominates the error ³².

A new inclusive analysis was presented by ALEPH which is the first evidence for semileptonic $b \rightarrow u$ transitions in b -hadrons produced at LEP ³³. ALEPH inclusively reconstructs the hadronic system accompanying the lepton in the semileptonic B decay and builds a set of kinematic variables to discriminate between $X_u \ell^- \bar{\nu}$ and $X_c \ell^- \bar{\nu}$ transitions by taking advantage of the different shape properties of these final states. The analysis is very aggressive, using a neural network technique to extract the inclusive $B \rightarrow X_u \ell^- \bar{\nu}$ branching ratio.

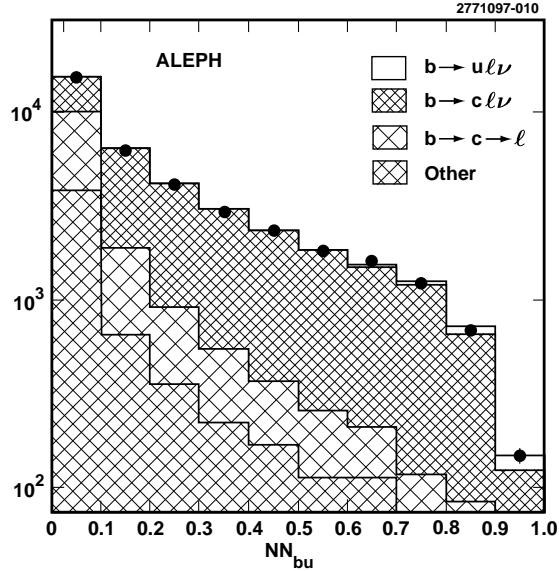


Figure 10: The neural net output indicating the presence of $b \rightarrow u\ell^{-}\bar{\nu}$ events in the ALEPH data.

An advantage of the technique is that it integrates over the entire lepton and hadron spectra for these decays, a technique not possible in $\Upsilon(4S)$ measurements, potentially reducing the model dependence of the result. A disadvantage is that the large background from $b \rightarrow c$ semileptonic decays needs to be understood at the one percent level for a meaningful extraction of $|V_{ub}|$ ³² since the boost of the B mesons at LEP is sufficient that even in the endpoint of the lepton spectrum, $b \rightarrow u\ell^{-}\bar{\nu}$ and $b \rightarrow c\ell^{-}\bar{\nu}$ events cannot be cleanly separated. Systematic errors on the analysis are still being evaluated; however, figure 10 shows the neural net output from the ALEPH analysis indicating the presence of a $b \rightarrow u\ell^{-}\bar{\nu}$ signal.

$|V_{ub}|$ has also been extracted from the exclusive decays $\bar{B} \rightarrow \pi\ell^{-}\bar{\nu}$ and $\bar{B} \rightarrow \rho\ell^{-}\bar{\nu}$ at CLEO that were first reported last year³⁴. From the exclusive $\bar{B} \rightarrow \pi\ell^{-}\bar{\nu}$ and $\bar{B} \rightarrow \rho\ell^{-}\bar{\nu}$ rates, the value is extracted:

$$|V_{ub}| = (3.3 \pm 0.2^{+0.3}_{-0.4} \pm 0.7) \times 10^{-3} \quad (6)$$

where the errors are statistical, experimental systematic, and theoretical model dependence respectively.

All $|V_{ub}|$ extractions rely heavily on models. The consistency of the results is very encouraging, but the large error bars are still dominated by theoretical uncertainties with poorly understood errors.

HQET and Charmless B Decays

Heavy quark symmetry is not obviously helpful in the analyses of semileptonic $b \rightarrow u$ decays since the light quark in the initial state is most certainly aware that the quark it is bound to

Table 6: Ratios of branching ratios for pseudoscalar to pseudoscalar semileptonic charm decays.

| Experiment | $\mathcal{B}(D^0 \rightarrow \pi^- \ell^+ \nu) / \mathcal{B}(D^0 \rightarrow K^- \ell^+ \nu)$ | $\mathcal{B}(D^+ \rightarrow \pi^0 \ell^+ \nu) / \mathcal{B}(D^+ \rightarrow \bar{K}^0 \ell^+ \nu)$ |
|------------------------|---|---|
| Mark III ³⁵ | $0.11^{+0.07}_{-0.04} \pm 0.02$ | |
| CLEO ³⁶ | $0.103 \pm 0.039 \pm 0.013$ | $0.046 \pm 0.014 \pm 0.017$ |
| E687 ³⁷ | $0.101 \pm 0.020 \pm 0.003$ | |

in the final state is no longer heavy. The overlap integral is analogous to the overlap between the electron wave function in hydrogen and in positronium. However, HQET can be used to relate the form factors for $c \rightarrow d$ semileptonic decays to those for $b \rightarrow u$ semileptonic decays at the same q^2 . In those two cases, the initial state and final state wave functions will be very similar. Since $|V_{cd}|$ is known from neutrino production of charm, form factors can be measured and models tested in charm decays and then extended to the B system to reduce theoretical errors on the $|V_{ub}|$ extraction ¹³.

New results in the charm sector from the fixed target experiments E687 and E791, as well as new CLEO results, have been encouraging. New measurements of $\mathcal{B}(D^0 \rightarrow \pi^- \ell^+ \nu)$ relative to $\mathcal{B}(D^0 \rightarrow K^- \ell^+ \nu)$ and $\mathcal{B}(D^+ \rightarrow \pi^0 \ell^+ \nu)$ relative to $\mathcal{B}(D^+ \rightarrow \bar{K}^0 \ell^+ \nu)$, as listed in table 6, can be used to extract the ratio of hadronic form factors for the pseudoscalar to pseudoscalar decays.

For the pseudoscalar to vector semileptonic decays, E791 reports a new measurement of the branching ratio $\mathcal{B}(D^+ \rightarrow \rho^0 \ell^+ \nu) / \mathcal{B}(D^+ \rightarrow \bar{K}^{*0} \ell^+ \nu)$ which is mainly sensitive to the A_1 form factor ³⁸. Figure 11 shows the very clean signals that are obtained with their 23 planes of high resolution silicon strips. The E791 and E687 results are beginning to discriminate among models, as summarized in table 7, that are also used to predict form factors for $b \rightarrow u$ semileptonic decays to extract $|V_{ub}|$. However, there is much more progress to be made and much larger data sets are needed before we will have a precision measurement of $|V_{ub}|$.

2.3 Puzzles in Semileptonic B Decay

There are 2 puzzles in semileptonic B decay. Neither is significant enough to rate the label of discrepancy and new results this year did not resolve either puzzle.

Puzzle 1

The first puzzle is that there has persistently been a difference in the semileptonic b branching ratios measured at the $\Upsilon(4S)$ and the Z with the value from LEP being higher as is

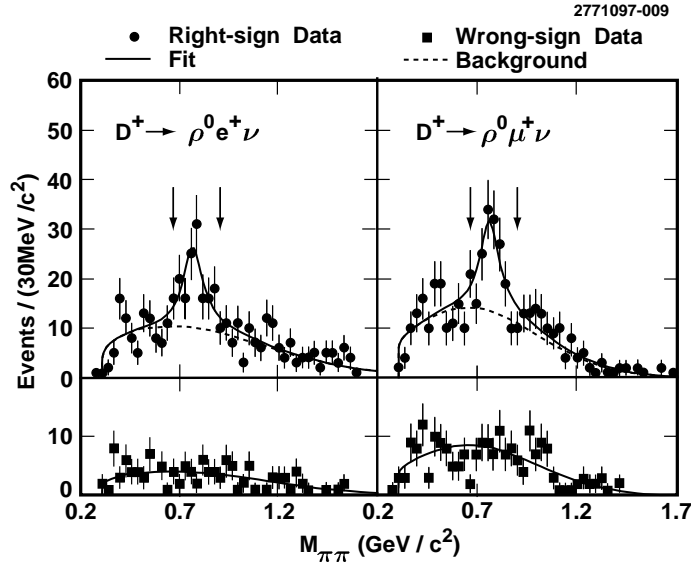


Figure 11: E791 signals for $D^+ \rightarrow \rho^0 \ell^+ \nu$.

evident in table 1. The ratio of branching ratios is

$$R = \frac{\mathcal{B}_{SL}^{4S}}{\mathcal{B}_{SL}^Z} = 0.930 \pm 0.046 \quad (7)$$

Given the short Λ_B hadron lifetimes measured at LEP, and if we assume that the semileptonic rates are similar for all species of B hadrons, we would actually expect the LEP value for the semileptonic b branching ratio to be lower than that measured at the $\Upsilon(4S)$, making the actual disagreement more severe. At this level of disagreement, about 2 standard deviations, one can only take a “wait and see” attitude. It is not clear if this is a problem or not.

Puzzle 2

The second puzzle is that historically, persisting to the present day, theoretical predictions of the semileptonic B branching ratio have been significantly larger than the experimentally measured values. The average experimental semileptonic branching ratios are given in table 1. Traditionally, the lower limit on the theoretical value for B_{SL} has been 12.5 percent ⁴⁶, which disagrees with the experimental values by many standard deviations.

If we believe the experimental numbers, and I do—they have been stable for a number of years and have been measured with a sufficient variety of techniques that it is hard to suspect serious experimental problems—then we must examine the ingredients of the theoretical calculations to see where the problem might lie.

We can write

Table 7: Ratios of rates for pseudoscalar to vector semileptonic charm decays. Most theoretical results are calculated for D^0 decays so following experimental references, the theoretical results for D^0 decay are compared to experimental results for D^+ decay using the relations: $\Gamma(D^+ \rightarrow \bar{K}^{*0} \ell^+ \nu) = \Gamma(D^0 \rightarrow K^{*-} \ell^+ \nu)$ and $\Gamma(D^+ \rightarrow \rho^0 \ell^+ \nu) = \frac{1}{2} \times \Gamma(D^0 \rightarrow \rho^- \ell^+ \nu)$.

| Experiment | $\mathcal{B}(D^+ \rightarrow \rho^0 \ell^+ \nu) / \mathcal{B}(D^+ \rightarrow \bar{K}^{*0} \ell^+ \nu)$ |
|--------------------------|---|
| E653 ³⁹ | $0.044_{-0.025}^{+0.031} \pm 0.014$ |
| E791 ³⁸ | 0.047 ± 0.013 |
| E687 ⁴⁰ | $0.073 \pm 0.019 \pm 0.013$ |
| Theory | $\mathcal{B}(D^+ \rightarrow \rho^0 \ell^+ \nu) / \mathcal{B}(D^+ \rightarrow \bar{K}^{*0} \ell^+ \nu)$ |
| ISGW2 ²⁴ | 0.022 |
| Jaus ⁴¹ | 0.030 |
| BSW ⁴³ | 0.037 |
| ELC ³⁰ | 0.047 ± 0.032 |
| APE ²⁷ | 0.043 ± 0.018 |
| UKQED ²⁹ | $0.036_{-0.013}^{+0.010}$ |
| LMMS ⁴⁴ | 0.040 ± 0.011 |
| Casalbuoni ⁴⁵ | 0.06 |

$$\mathcal{B}_{SL} = \frac{\Gamma_{\text{semi-leptonic}}}{\Gamma_{\text{semi-leptonic}} + \Gamma_{\text{hadronic}} + \Gamma_{\text{leptonic}}}. \quad (8)$$

Γ_{leptonic} is very small, and I have argued that we understand the semileptonic rate so the likely culprit is a flaw in our understanding of Γ_{hadronic} for B meson decays.

If we break hadronic rate into its constituent pieces, we have $\Gamma_{\text{hadronic}}(b) = \Gamma(b \rightarrow c\bar{u}d) + \Gamma(b \rightarrow c\bar{c}s) + \Gamma(b \rightarrow sg)$ (g here refers to *glue*) and a variety of calculations have examined these component rates in detail. Note that to reduce the expectation for the semileptonic branching ratio from 12.5 % to the experimental value of 10-11% requires a 20% enhancement of Γ_{hadronic} so we presumably are not looking for something terribly subtle!

Theoretical solutions to the problem fall into four categories.

1. There could be an enhancement of $\Gamma(b \rightarrow c\bar{u}d)$ due to non-perturbative effects. The problem with this class of solutions is that it predicts $\tau_{B^+}/\tau_{B^0} \sim 0.8$,⁴⁷ which is not a comfortable fit to the experimental lifetime ratio of 1.06 ± 0.04 ¹⁹.

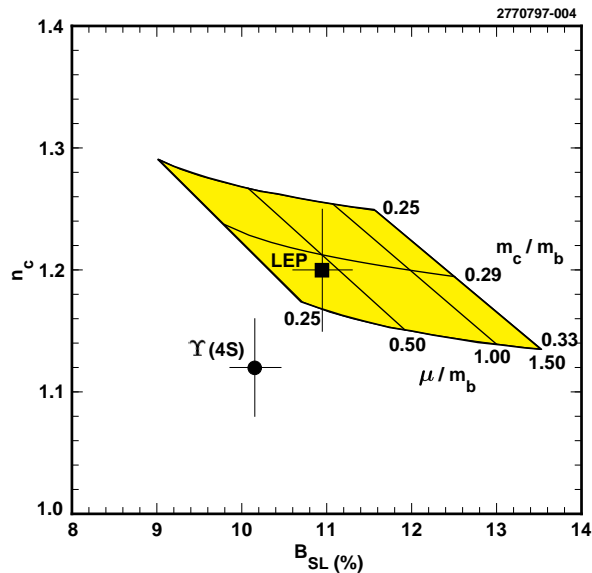


Figure 12: The number of charm quarks per b decay vs. the semileptonic branching ratio. The theoretical curves are from Neubert and Sachrajda⁴⁹. The experimental values are the averages compiled for this review.

2. There could be an enhancement of $\Gamma(b \rightarrow c\bar{c}s)$ due to large QCD corrections. The problem with this solution is that it affects another experimental quantity, n_c , which is the average number of charm or anticharm quarks per b decay. Theoretical models that significantly increase $\Gamma(b \rightarrow c\bar{c}s)$ to bring the semileptonic branching ratio into line with experiment find n_c in the range of 1.2 to 1.3^{48,49}.

Experimentally, n_c looks to be lower than the theoretical values although when both theoretical errors and experimental errors are included, this solution looks appealing as summarized in figure 12. However, it is important to note that the measurements that make up n_c are in disagreement with each other at roughly the 2 sigma level in how many D mesons there are per b decay, so that it is perhaps premature to talk about either agreeing or disagreeing with theory at this point.

Table 8 lists the branching ratios from LEP and from CLEO that are summed to extract n_c . We see that there are more D_s 's and charm-baryons per b quark at LEP as to be expected, since at LEP the b quark forms a B_s or Λ_b a fraction $f_{b \rightarrow B_s}$ or $f_{b \rightarrow \Lambda_B}$ of the time. At CLEO, only B_u and B_d can be produced. What is problematic is that one would expect to see fewer D mesons per b decay at LEP (for just the same reason...since b quarks are forming B_s or Λ_b , then only a fraction of the b quarks, $f_{b \rightarrow B}$, are making B_u and B_d which decay dominantly to D mesons) and the measured rates for $b \rightarrow DX$ at CLEO and LEP don't show enough difference. The numbers are too close, if we assume the traditional values $f_{b \rightarrow B} = 0.378 \pm 0.022$, $f_{b \rightarrow B_s} = 0.112 \pm 0.019$, and $f_{b \rightarrow \Lambda_B} = 0.132 \pm 0.041$ ⁵⁰!

I estimate this discrepancy to be at the 1.8 σ level when I carefully include all errors (correlated and uncorrelated) and scale the experimental results to common D branching

Table 8: Summary of the branching ratios used in the calculation of n_c . The $\Upsilon(4S)$ branching ratios are from CLEO^{53,54,55}. The LEP branching ratios are averaged over the four LEP experiments with careful attention to correlated systematic errors⁵⁶, and all branching ratios are scaled to the normalizing branching ratios listed in table 9.

| | $\Upsilon(4S)$ | LEP |
|--|-------------------|-------------------|
| $\mathcal{B}(b \rightarrow D^0 X)$ | 0.642 ± 0.030 | 0.576 ± 0.026 |
| $\mathcal{B}(b \rightarrow D^+ X)$ | 0.246 ± 0.021 | 0.224 ± 0.019 |
| $\mathcal{B}(b \rightarrow D_s^+ X)$ | 0.118 ± 0.031 | 0.191 ± 0.050 |
| $\mathcal{B}(b \rightarrow \Lambda_C^+ X)$ | 0.039 ± 0.020 | 0.114 ± 0.020 |
| $\mathcal{B}(b \rightarrow \Xi_c X)$ | 0.020 ± 0.010 | 0.063 ± 0.021 |
| $\mathcal{B}(b \rightarrow (c\bar{c})X)$ | 0.054 ± 0.007 | 0.034 ± 0.012 |
| $n_c = \Sigma \mathcal{B}_i$ | 1.119 ± 0.053 | 1.202 ± 0.067 |

Table 9: Summary of the normalizing D branching ratios used in the calculation of n_c .

| | |
|---|---------------------|
| $\mathcal{B}(D^0 \rightarrow K^- \pi^+)$ ⁴ | 0.0388 ± 0.0010 |
| $\mathcal{B}(D^+ \rightarrow K^- \pi^+ \pi^+)$ ⁴ | 0.088 ± 0.006 |
| $\mathcal{B}(D_s^+ \rightarrow \phi \pi^+)$ ⁵⁰ | 0.036 ± 0.009 |

ratios as listed in table 9.

This discrepancy is just at the level that it might make you uncomfortable and it is certainly in need of resolution before the experimentalists can claim any serious conflicts with theory.

One implication, if this discrepancy holds up under further investigation, is that perhaps there is an error in our understanding of how often the b quark makes a B meson at LEP! Turning the comparison of these branching ratios into a measurement of $f_{b \rightarrow B}$ gives $f_{b \rightarrow B} = 0.45 \pm 0.03$ to be compared with 0.378 ± 0.022 which is traditionally used. It is amusing to note that new measurements of $f_{b \rightarrow B}$ reported at this conference are helpful in resolving this problem¹⁹.

3. In a variation on the previous solution to the problem, it has been suggested that a sizable fraction of $b \rightarrow c\bar{c}s$ transitions could appear as $b \rightarrow$ no open charm⁵¹. The hypothesis is that a large component of low mass $c\bar{c}$ pairs are seen as light hadrons and not as open charm. n_c would not be increased by this mechanism, and this possibility

is currently under experimental investigation.

4. The most intriguing possibility for solving the semileptonic branching ratio experimental shortfall is an enhancement of $\Gamma(b \rightarrow sg)$ from some unexpected source of new physics.

Theorists also point out a fifth solution.

5. There could be a systematic experimental problem. One place attention has focussed is on the $D^0 \rightarrow K^-\pi^+$ branching ratio ⁵².

Experimental Attempts to Resolve Puzzles in Semileptonic B Decays

Given no compelling theoretical resolution to the puzzles in the semileptonic rate, a variety of experiments in the last year have attempted to address the issue. The most comprehensive new studies are done by CLEO ⁵⁷ and DELPHI ⁵⁸.

CLEO uses lepton- D charge and angular correlations to extract rates for $\bar{B} \rightarrow DX$, $\bar{B} \rightarrow \bar{D}X$, and $\bar{B} \rightarrow DX\ell^-\bar{\nu}$. With these three measurements, three unknowns can be extracted:

1. the number of D 's produced at the upper vertex in B decay: $\mathcal{B}(B \rightarrow DX) = 0.079 \pm 0.022$
2. $\mathcal{B}(b \rightarrow sg) = 0.002 \pm 0.040$ or < 0.068 at 90% confidence level, and
3. $\mathcal{B}(D^0 \rightarrow K^-\pi^+) = 0.0369 \pm 0.0020$.

The new CLEO measurement of $\mathcal{B}(B \rightarrow DX)$ gives $\mathcal{B}(b \rightarrow c\bar{c}s) = \mathcal{B}(b \rightarrow (c\bar{c})s) + \mathcal{B}(b \rightarrow cD_s) + \mathcal{B}(b \rightarrow \text{charm} - \text{baryons}) + \mathcal{B}(b \rightarrow DX) = 0.219 \pm 0.036$, in good agreement with theoretical expectation. The $D^0 \rightarrow K^-\pi^+$ branching ratio extracted from the analysis is in good agreement with the world average listed in table 9 and another new CLEO measurement of the same branching ratio using a partial reconstruction technique ⁵⁹, and the new limit on $b \rightarrow sg$ neither supports nor rules out the possibility of new physics.

The new DELPHI analysis fits to the b quark tagging probability distribution to contributions from events with 0 charmed particles, 1 charmed particle or 2 charmed particles, where the different final states can be distinguished since they have different numbers of secondary vertices in the final state. DELPHI extracts the branching ratio to 0 charm (no open charm) in the final state, and the branching ratio to 2 charm particles in the final state. By subtracting the Standard Model expectation for the branching ratio to no open charm, they put a limit on new physics producing no open charm of 4.5% at the 95% confidence level.

What do we conclude? I feel put in a miserable position as a reviewer since I can conclude nothing. I am actually not totally convinced there is a problem when all errors, both theoretical and experimental are included. Radical theoretical solutions seem experimentally unacceptable. Experimental probes of the components that go into making up the rate see some experimental problems, but no solutions to the overall problem. There is no evidence for new physics and no conclusive possibility of ruling it out. To nail this down and resolve this messy issue in a satisfactory manner will require more data.

3 Heavy Quarks Beyond Tree Level

So far, I have been concentrating on heavy meson decays at tree level. I now want to switch to discussing heavy meson decays beyond tree level and rare decays. I want to take a few minutes to stress the importance of these decays, particularly in the B sector.

Rare processes, for which the Standard Model expectation for the rate is small, can be used to probe new physics. Those processes that are highly suppressed or explicitly forbidden to first order in the Standard Model are especially sensitive since often new physics can compete favorably. The other interest in B decays beyond tree level is that they offer methods for determining the phases of the elements of the CKM matrix, thereby probing the Standard Model mechanism for CP violation.

I want to stress that in contrast to the results that dominated the first part of this review, the new results on hadronic rare B decays are full of surprises. While we can start to observe overall patterns, the patterns are largely unexplained.

3.1 Rare Hadronic B Decays

This year has seen a flood of new results on rare B decays, especially from the CLEO experiment. Where previously there were upper limits, now in many cases there are signals. Particularly for the hadronic rare B decays, there have been significant improvements in analysis techniques. However, the dominant improvement has been the addition of more data so that the new results presented this year are based on the full $3.3 \times 10^6 B\bar{B}$ of the CLEO II data set.

$B \rightarrow \pi\pi/\pi K/KK$

Let me start by discussing the new CLEO results on the $B \rightarrow \pi\pi/K\pi/KK$ decay modes. Many diagrams contribute to these decays as illustrated in figure 13, but penguin and tree diagrams are expected to dominate.

The CLEO analysis looks in $\Upsilon(4S)$ decays for two stiff back-to-back particles. The dominant backgrounds are $e^+e^- \rightarrow q\bar{q}$ from the continuum under the $\Upsilon(4S)$ resonance with continuum charm accounting for about 25 percent of the background. Yields are extracted from a likelihood fit to the data and branching ratios are calculated:

$$\mathcal{B}(B^0 \rightarrow K^+\pi^-) = \left(1.5_{-0.4-0.1}^{+0.5+0.1} \pm 0.1\right) \times 10^{-5} \quad (9)$$

$$\mathcal{B}(B^0 \rightarrow \pi^+\pi^-) < 1.5 \times 10^{-5} \quad (90\%c.l.) \quad (10)$$

$$\mathcal{B}(B^0 \rightarrow K^+K^-) < 0.4 \times 10^{-5} \quad (90\%c.l.) \quad (11)$$

Similar analyses yield significant signals in $B^+ \rightarrow \pi^+K^0$ and in $B^+ \rightarrow (\pi^+\pi^0 + K^+\pi^0)$, which is denoted $B \rightarrow h^+\pi^0$. These results are summarized in table 10. Also indicated are the dominant amplitudes thought to be contributing to each decay ⁶⁰. Figure 14 shows the projections in reconstructed B mass for the signals.

The observation of $B \rightarrow K^0\pi^+$ is interesting because it directly measures the strength of the gluonic penguin. The observed rate is about a factor of two higher than expected. This

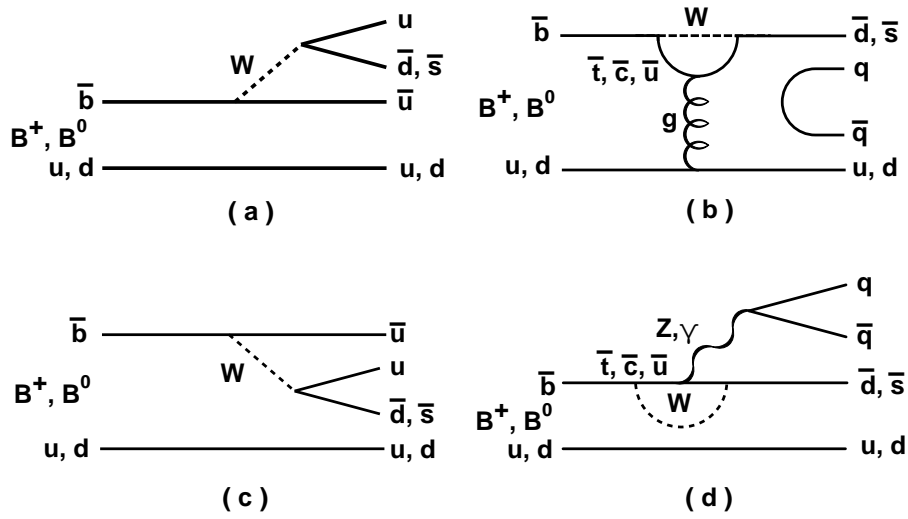


Figure 13: Feynman diagrams illustrating the dominant decay processes that contribute to the $B \rightarrow \pi\pi/K\pi$ decays: (a) external W -emission, (b) gluonic penguin, (c) internal W -emission, and (d) external electroweak penguin.

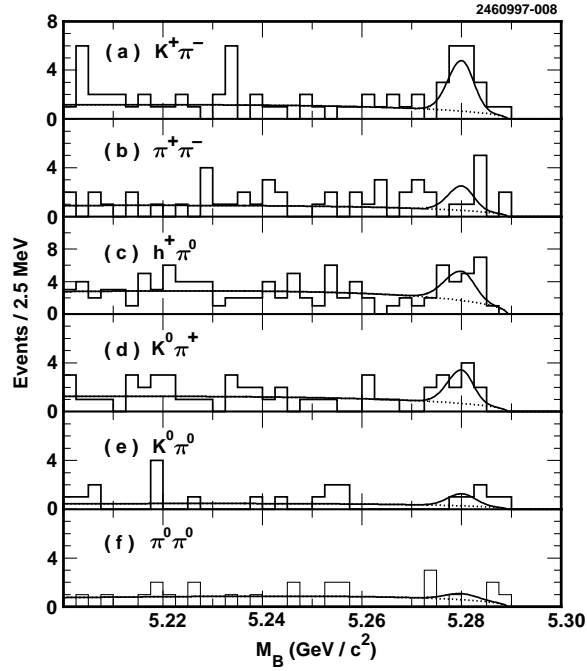


Figure 14: Reconstructed B mass plots for CLEO data (a) $B^0 \rightarrow K^+\pi^-$, (b) $B^0 \rightarrow \pi^+\pi^-$, (c) $B^+ \rightarrow h^+\pi^0$, (d) $B^+ \rightarrow \pi^+K^0$, (e) $B^0 \rightarrow K^0\pi^0$, and (f) $B^0 \rightarrow \pi^0\pi^0$. The data are the histogram and the scaled projection of the total likelihood fit (solid curve) and the continuum background (dotted curve) are overlaid. h^+ indicates K^+ or π^+ .

Table 10: Summary of the new CLEO results on the $B \rightarrow K\pi/\pi\pi/K\pi$ branching ratios. The second column indicates the dominant amplitudes for each decay using the notation of Gronau *et al.* ⁶⁰. Upper limits are quoted at 90 % confidence level. h^\pm indicates π^\pm or K^\pm .

| Mode | Amplitude | $\mathcal{B}(10^{-5})$ |
|--------------------------------|----------------------------|-------------------------------------|
| $B \rightarrow K^\pm\pi^\pm$ | $-(T' + P')$ | $1.5^{+0.5+0.1}_{-0.4-0.1} \pm 0.1$ |
| $B \rightarrow K^\pm\pi^0$ | $-(T' + C' + P')/\sqrt{2}$ | < 1.6 |
| $B \rightarrow K^0\pi^\pm$ | P' | $2.3^{+1.1+0.3}_{-1.0-0.3} \pm 0.2$ |
| $B \rightarrow K^0\pi^0$ | $-(C' - P')/\sqrt{2}$ | < 4.1 |
| $B \rightarrow \pi^\pm\pi^\mp$ | $-(T + P)$ | < 1.5 |
| $B \rightarrow \pi^\pm\pi^0$ | $-(T + C)/\sqrt{2}$ | < 2.0 |
| $B \rightarrow \pi^0\pi^0$ | $-(C - P)/\sqrt{2}$ | < 0.9 |
| $B \rightarrow K^\pm K^\mp$ | E | < 0.4 |
| $B \rightarrow K^\pm K^0$ | P | < 2.1 |
| $B \rightarrow K^0 \bar{K}^0$ | P | < 1.7 |
| $B \rightarrow h^\pm\pi^0$ | | $1.6^{+0.6+0.3}_{-0.5-0.2} \pm 0.2$ |
| $B \rightarrow h^\pm K^0$ | | $2.4^{+1.1+0.2}_{-0.9-0.2} \pm 0.2$ |

is our first surprise. We now can look at $B \rightarrow K^\pm\pi^\mp$ which both the tree and penguin can contribute to. The fact that the branching ratio is smaller than $B \rightarrow \pi^+K^0$ may indicate interference and Fleischer has used this to draw tentative conclusions about γ , the phase of V_{ub} , although statistical errors are very large still ⁶¹. The branching ratio for $B \rightarrow \pi^\pm\pi^\mp$ is small compared to expectation, and there is no explanation why it is low. Perhaps it is a fluctuation since in comparison with $B \rightarrow \pi^+\pi^0$ we expect twice the rate. The $B \rightarrow KK$ modes are the one place where there are no surprises. We do not expect much, and we do not see much.

I want to briefly mention that both ALEPH and DELPHI have statistically significant signals in the sum of $B^0 \rightarrow (K^+\pi^- + \pi^+\pi^-)$ that are consistent with and less precise than new CLEO results ⁶².

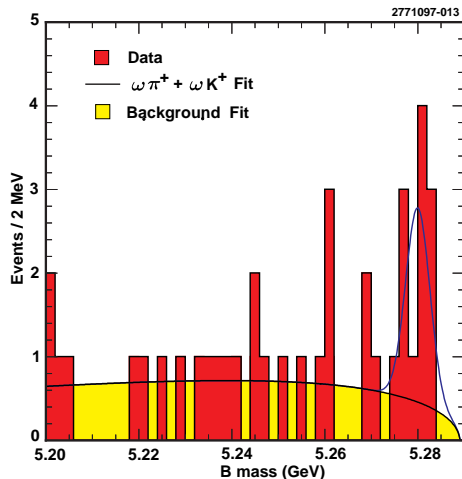


Figure 15: Reconstructed B mass plots for CLEO data in the channel $B^+ \rightarrow \omega\pi^+ + \omega K^+$.

Other Rare Hadronic B decays

The pattern of the hadronic penguin decays of the B meson appearing at a rate exceeding naive expectation continues. Signals are evident in $B^+ \rightarrow \omega\pi^+ + \omega K^+$ and there is a stunning signal in $B^+ \rightarrow \eta' K^+$ as shown in figures 15 and 16. The measured branching ratios from CLEO are still preliminary ^{63,64}:

$$\mathcal{B}(B^+ \rightarrow \omega K^+) = \left(1.5_{-0.6}^{+0.7} \pm 0.3\right) \times 10^{-5} \quad (12)$$

$$\mathcal{B}(B^+ \rightarrow \omega\pi^+) = \left(1.1_{-0.5}^{+0.6} \pm 0.2\right) \times 10^{-5} \quad (13)$$

$$\mathcal{B}(B^+ \rightarrow \eta' K^+) = \left(7.1_{-2.1}^{+2.5} \pm 0.9\right) \times 10^{-5} \quad (14)$$

$$\mathcal{B}(B^+ \rightarrow \eta'\pi^+) < 4.5 \times 10^{-5} \quad (90\%c.l.) \quad (15)$$

$$\mathcal{B}(B^+ \rightarrow \eta h^+) < 0.8 \times 10^{-5} \quad (90\%c.l.) \quad (16)$$

The amplitudes for these decays all have many contributions with the expectation that $B^+ \rightarrow \omega K^+$, $B^+ \rightarrow \eta K^+$ and $B^+ \rightarrow \eta' K^+$ are dominated by the gluonic penguin diagram. The $B^+ \rightarrow \omega\pi^+$, $B^+ \rightarrow \eta\pi^+$ and $B^+ \rightarrow \eta'\pi^+$ modes are expected to be dominated by tree diagrams. The rate for the decay $B^+ \rightarrow \eta' K^+$ is so large it deserves special note. Even relative to other gluonic penguins such as $B \rightarrow K\pi$ which are larger than expected at the 1.5×10^{-5} level, the branching ratio of 7×10^{-5} is so significant that many have speculated that there must be other contributions to the rate than just the Standard Model penguin. This is further supported by evidence of anomalously large inclusive branching ratio for $B \rightarrow \eta' X_s$ ⁶⁵:

$$\mathcal{B}(B \rightarrow \eta' X_s) = (6.2 \pm 1.6 \pm 1.3) \times 10^{-4}; \quad 2.0 < p_{\eta'} < 2.7\text{GeV} \quad (17)$$

What could be going on? The most obvious trend is that the gluonic penguins are larger than we thought. This pattern seems to pervade rare B decays. The fact that $B^+ \rightarrow \eta' K^+$

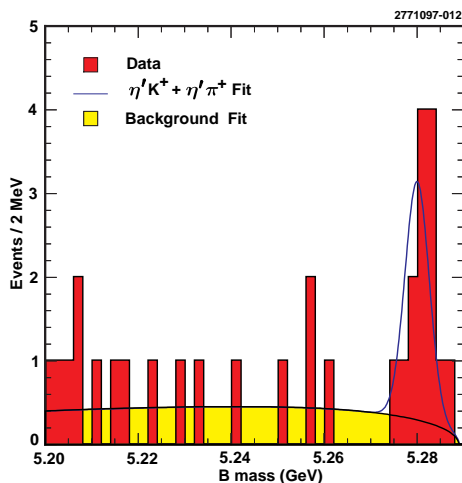


Figure 16: Reconstructed B mass plots for CLEO data in the channel $B^+ \rightarrow \eta' \pi^+ + \eta' K^+$.

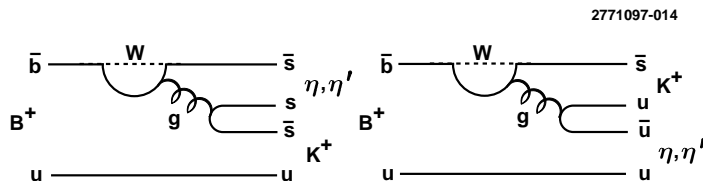


Figure 17: Two penguin diagrams for the $B^+ \rightarrow \eta/\eta' K^+$ modes. Constructive interference between the two diagrams enhances the $\eta' K^+$ final state and destructive interference suppresses the ηK^+ final state.

is so much larger than $B^+ \rightarrow \eta K^+$ was not totally unexpected⁶⁶ and is thought to be due to the interference of the 2 penguin diagrams shown in figure 17 with $g \rightarrow u\bar{u}$ and $g \rightarrow s\bar{s}$. However, the overall enhancement of the η' modes has fueled quite a lot of theoretical speculation⁶⁷, including unexpected enhancement of the hairpin diagram or a source of η' from $b \rightarrow c\bar{c}s$ decays as schematically illustrated in figure 18. This latter source of speculation is particularly attractive since it helps to explain the low value of $\mathcal{B}(B \rightarrow X\ell\nu)$ which we worried about earlier. At this moment, speculation is rampant and time and more data will be needed to sort this out. It is worth pointing out that enhanced gluonic penguins could be both a blessing and a curse to studies of CP violation in B decays. They can be a source of complication for modes we had hoped were clean. However, they may also offer more opportunities for studying CP violation in B decays than previously realized.

3.2 Effective Flavor Changing Neutral Currents

I now want to turn to a class of beyond tree level process in heavy quark decay that can be described generically as effective flavor changing neutral current (FCNC) processes. This includes decays like $b \rightarrow s\gamma$, $b \rightarrow s\ell^+\ell^-$, $B \rightarrow K^{(*)}\ell^+\ell^-$ and $D \rightarrow X\ell^+\ell^-$. These decays are dominated by electromagnetic and electroweak penguins. There are no competing tree

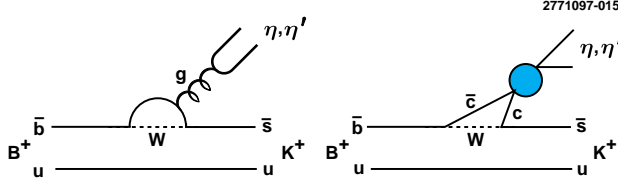


Figure 18: Two possible explanations for the unexpected enhancement of $B \rightarrow \eta' X$ are illustrated.

level processes as was the case for the gluonic penguins, so these penguin and box diagrams offer clean experimental handles for probing loops in the decays of heavy quarks. This year saw many new results in charm and bottom decays from the LEP experiments, CDF and D0, CLEO, E687 and E791.

The effective FCNC decays in charm are very interesting if one sees a signal, which no one does. Unfortunately, the GIM mechanism which is effective in suppressing the Standard Model rates for loop level charm decays also effectively suppresses many non-Standard Model rates, and so rare charm decays are not particularly sensitive as probes of ‘standard’ new physics. However, one can always be surprised! Limits from E687 and E791 are in the range of $10 - 20 \times 10^{-5}$ with Standard Model rates for these decays predicted to be much smaller – typically or order 10^{-10} .

In bottom decays, the experimental sensitivity to loop processes is somewhat better than in charm decays, depending on the mode. Because the GIM mechanism is not particularly effective in B decays due to the very large top quark mass, Standard Model rates are accessible and many non-Standard Model rates are potentially accessible as well. Signals are seen in some of the electromagnetic penguin modes, and both signal rates and upper limits for FCNC decays are useful for putting significant model dependent constraints on extensions of the Standard Model such as supersymmetry. The disadvantage of studying FCNC decays in the bottom system relative to charm is that if one sees a signal, a good calculation of the expected Standard Model rate is needed. One must look for deviations from the Standard Model rate to search for evidence of new physics.

The electromagnetic penguin $b \rightarrow s\gamma$ has now been seen in both exclusive and inclusive channels. The exclusive decay $B \rightarrow K^*\gamma$ has been observed by the CLEO experiment ⁶⁸ with an upper limit placed on the exclusive $B_s \rightarrow \phi\gamma$ penguin decays from ALEPH ⁶⁹.

$$\mathcal{B}(B \rightarrow K^*\gamma) = (4.2 \pm 0.8 \pm 0.6) \times 10^{-5} \text{ (CLEO)} \quad (18)$$

$$\mathcal{B}(B_s \rightarrow \phi\gamma) < 29 \times 10^{-5} \text{ 90\%c.l. (ALEPH)} \quad (19)$$

The more interesting channel is the inclusive electromagnetic penguin where calculations are thought to be much more reliable. CLEO first observed the inclusive electromagnetic penguin decay ⁷⁰ and ALEPH has recently reported a preliminary observation of this decay ⁷¹.

$$\mathcal{B}(B \rightarrow s\gamma) = (2.32 \pm 0.57 \pm 0.35) \times 10^{-4} \text{ (CLEO)} \quad (20)$$

$$\mathcal{B}(B \rightarrow s\gamma) = (3.38 \pm 0.74 \pm 0.85) \times 10^{-4} \text{ (ALEPH)} \quad (21)$$

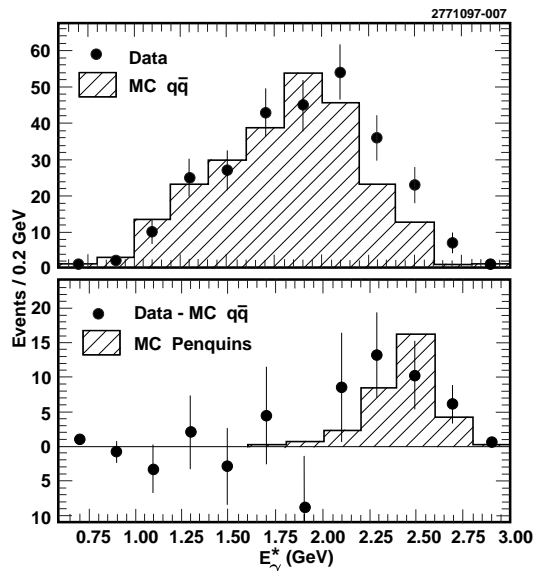


Figure 19: The photon spectrum showing the signal for $b \rightarrow s\gamma$ from ALEPH. The top plot shows the raw photon spectrum. The points are data and the histogram is Monte Carlo expectation with no penguin contribution. In the bottom plot the Monte Carlo photon spectrum for photons from all other sources has been subtracted showing the signal for the penguin decay. The points are again data and the histogram is the expectation of the photon spectrum for $b \rightarrow s\gamma$ decays from Monte Carlo.

The ALEPH analysis takes advantage of the long flight of the B meson at LEP to tag a b jet in one hemisphere and then requires a high energy photon in the opposite hemisphere. They use rapidity, momentum and impact parameter to discriminate tracks produced in the b decay from tracks from primary hadronization. In this way they inclusively reconstruct the candidate B meson mass. After assorted cuts, they fit the photon energy distribution in the B candidate rest frame to extract the $b \rightarrow s\gamma$ rate. The photon spectrum from the ALEPH analysis is shown in figure 19.

Dramatic progress has been made in the theoretical interpretation of the inclusive electromagnetic penguin decays where two new calculations of the $b \rightarrow s\gamma$ rate now include all terms to next-to-leading order ^{72,73}. The new calculations give a slightly increased theoretical Standard Model rate for the process and substantially reduce the theoretical errors. This results in tighter (although still model dependent) constraints on new physics from this decay rate.

The other particularly interesting FCNC decays are the decays with a lepton pair in the final state. No one has yet seen a signal. The recent results on these decays are summarized in table 11. The interesting point to note here is that a wide variety of experiments are now within an order of magnitude of the Standard Model expectation for these decays.

Figure 20 illustrates the power of the effective FCNC decays. The shaded areas are the regions of parameter space that are excluded for two generic types of models that have extra Higgs. SUSY is an example of type II, but the limits shown here assume that the charged Higgs and nothing else is affecting the $b \rightarrow s\gamma$ rate. The limits are powerful, but

Table 11: Summary of the recent results on effective flavor changing neutral currents in B and D decay. The experimental results on the branching ratios are given along with the theoretical expectation in the Standard Model.

| Mode | \mathcal{B}_{expt} (10^{-5}) | Expt. | \mathcal{B}_{th} (10^{-5}) |
|-----------------------------------|---------------------------------------|-----------------------------|-------------------------------------|
| $b \rightarrow s\gamma$ | 25.5 ± 6.1 | CLEO/ALEPH ^{70,71} | 34 ± 3 ^{72,73} |
| $B \rightarrow Ke^+e^-$ | < 1.2 | CLEO ⁷⁴ | $0.02 - 0.05$ ⁷⁵ |
| $B \rightarrow K\mu^+\mu^-$ | < 0.9 | CLEO ⁷⁴ | $0.02 - 0.05$ ⁷⁵ |
| $B \rightarrow K^*e^+e^-$ | < 1.6 | CLEO ⁷⁴ | $0.2 - 0.5$ ⁷⁵ |
| $B \rightarrow K^*\mu^+\mu^-$ | < 2.5 | CDF ⁷⁶ | $0.2 - 0.5$ ⁷⁵ |
| $b \rightarrow s\mu^+\mu^-$ | < 5.8 | CLEO ⁷⁷ | 0.6 ⁷⁸ |
| $b \rightarrow se^+e^-$ | < 5.7 | CLEO ⁷⁷ | 0.8 ⁷⁸ |
| $b \rightarrow s\nu\bar{\nu}$ | < 77 | ALEPH ⁷⁹ | 4 ⁸⁰ |
| $B_d \rightarrow \mu^+\mu^-$ | < 0.026 | CDF ⁸¹ | ~ 0.00001 ⁷⁵ |
| $B_s \rightarrow \mu^+\mu^-$ | < 0.077 | CDF ⁸¹ | ~ 0.0001 ⁷⁵ |
| $D^+ \rightarrow \pi^+e^+e^-$ | < 6.6 | E791 ⁸² | < 0.001 ⁸⁴ |
| $D^+ \rightarrow \pi^+\mu^+\mu^-$ | < 1.8 | E791 ⁸² | < 0.001 ⁸⁴ |
| $D^+ \rightarrow K^+e^+e^-$ | < 20 | E687 ⁸³ | $< 10^{-10}$ ⁸⁴ |
| $D^+ \rightarrow K^+\mu^+\mu^-$ | < 9.7 | E687 ⁸³ | $< 10^{-10}$ ⁸⁴ |

they are also (with the exception of the LEP direct limits) model dependent ⁸⁵.

Another way to present the constraints from the FCNC decays is to show how they restrict the $WW\gamma$ anomalous couplings. In figure 21, the region allowed by $b \rightarrow s\gamma$ cuts an impressive swath across the region allowed by $D0$ from its analysis of $p\bar{p} \rightarrow W\gamma X$ ⁸⁵.

4 Conclusions

Summarizing the status of heavy quark decays, the tree level processes are reasonably well understood, but we need to understand them even better if we want to improve our knowledge of $|V_{ub}|$ and $|V_{cb}|$. More data in both charm and bottom decays will be necessary to accomplish this. There is no strong evidence of any serious misunderstanding in the tree level decays. There are a variety of 2σ problems that either need to become 3σ problems or go away!

The field of heavy quark decays beyond tree level is emerging and rapidly developing. There have been many surprises in the hadronic rare B decays. The gluonic penguins seem to be consistently larger than expected. The FCNC decays are providing substantial (although model dependent) constraints on new physics. However, the goal of studying the phases of elements of the CKM matrix is still a ways off. I think that we can eagerly look

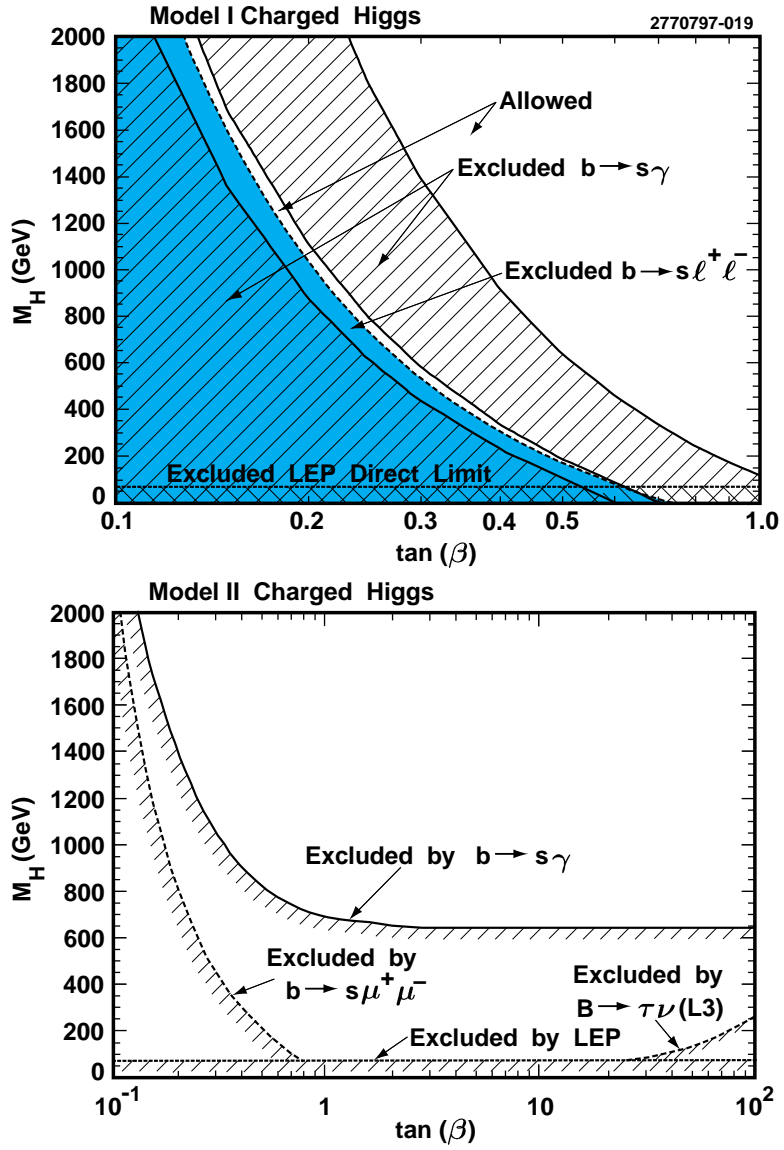


Figure 20: The parameter space for two generic models with extra Higgs is shown with the areas excluded by the FCNC results shaded. The LEP direct limit is also shown.

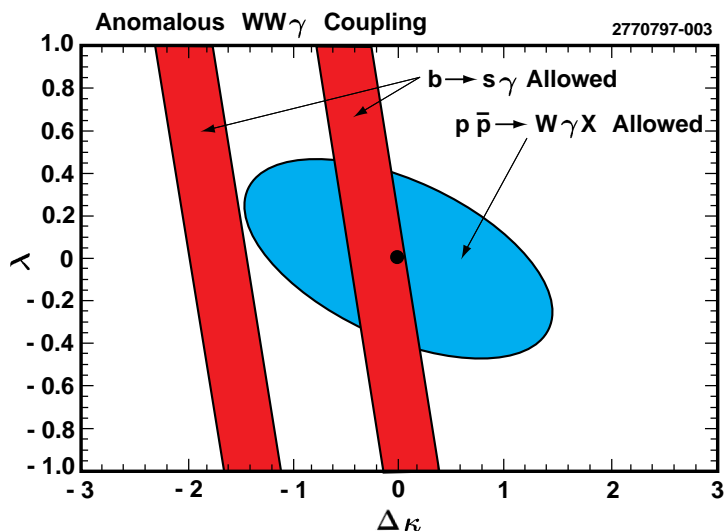


Figure 21: The allowed values for $WW\gamma$ anomalous couplings from the measured $b \rightarrow s\gamma$ branching ratio and the $D0$ result on $p\bar{p} \rightarrow W\gamma X$ are shown as shaded regions.

forward to the Lepton–Photon Conference perhaps 4 years from now when data will be starting to probe the CKM phases. We are at the beginning of a new era in heavy quark physics with studies of rare processes. I look forward to exploring where it leads us.

Acknowledgments

Many people were generous with their time and effort in helping me to prepare this review. I am particularly indebted to David Cassel who provided the branching ratio averages for the semileptonic B decays. Lawrence Gibbons and Ken Bloom graciously supplied the new $|V_{cb}|$ averages. Claudia Glasman was a wonderful scientific secretary. I am grateful to Veronique Boisvert, David Crowcroft, and Andy Foland who read the manuscript carefully and made many thoughtful comments. This work was supported by the National Science Foundation.

References

1. G. Goldhaber *et al.* (MARKI), *Phys. Rev. Lett.* **37**, 255 (1976).
2. R. D. Schamberger in *Proceedings of the 10th International Symposium on Lepton and Photon Interactions at High Energies*, Bonn, Germany, August, 1981.
3. N. Cabibbo, *Phys. Rev. Lett.* **10**, 531 (1963); M. Kobayashi and T. Maskawa, *Prog. Theor. Phys.* **49**, 652 (1973).
4. J. D. Richman in *Proceedings of the 28th International Conference on High Energy Physics*, Warsaw, Poland, July 1994.
5. L. K. Gibbons in *Proceedings of the 28th International Conference on High Energy Physics*, Warsaw, Poland, July 1994.

6. H. Albrecht *et al.* (ARGUS), *Phys. Lett. B* **318**, 397 (1993); B. Barish *et al.* (CLEO), *Phys. Rev. Lett.* **76**, 1570 (1996).
7. D. Buskulic *et al.* (ALEPH), EPS-0404, Contributed to *International Europhysics Conference on High Energy Physics*, Brussels, Belgium, 1995; P. Abreu *et al.* (DELPHI), *Z. Phys. C* **66**, 323 (1995); M. Acciarri *et al.* (L3), *Z. Phys. C* **71**, 379 (1996); R. Akers *et al.* (OPAL), *Z. Phys. C* **60**, 199 (1993).
8. D. Buskulic *et al.* (ALEPH), *Phys. Lett. B* **395**, 373 (1997); H. Albrecht *et al.* (ARGUS), *Phys. Lett. B* **229**, 175 (1989); M. Athanas *et al.* (CLEO), *Phys. Rev. Lett.* **79**, 2208 (1997); H. Albrecht *et al.* (ARGUS), DESY 92-29, 1992.
9. H. Albrecht *et al.* (ARGUS), *Z. Phys. C* **57**, 533 (1993); H. Albrecht *et al.* (ARGUS), *Phys. Lett. B* **324**, 249 (1994); H. Albrecht *et al.* (ARGUS), *Phys. Lett. B* **275**, 195 (1992); D. Bortoletto *et al.* (CLEO), *Phys. Rev. Lett.* **63**, 1667 (1989).
10. B. Barish *et al.* (CLEO), *Phys. Rev. D* **51**, 1014 (1995); D. Buskulic *et al.* (ALEPH), *Phys. Lett. B* **395**, 373 (1997); P. Abreu *et al.* (DELPHI), *Z. Phys. C* **71**, 539 (1996); K. Ackerstaff *et al.* (OPAL), *Phys. Lett. B* **395**, 128 (1997); H. Albrecht *et al.* (ARGUS), *Phys.Rept.* **276**, 223 (1996).
11. D. Buskulic *et al.* (ALEPH), *Z.Phys.C* **73**, 601 (1997)
12. A. Anastassov *et al.* (CLEO), CLNS 97-17 (1997).
13. N. Isgur and M. B. Wise, *Phys. Lett. B* **232**, 113 (1989); N. Isgur and M. B. Wise, *Phys. Lett. B* **237**, 527 (1990); E. Eichten and B. Hill, *Phys. Lett. B* **234**, 511 (1990); H. Georgi, *Phys. Lett. B* **240**, 447 (1990).
14. M. Neubert, *Phys. Lett. B* **264**, 455 (1991).
15. A. Czarnecki, *Phys. Rev. Lett.* **76**, 4124 (1996).
16. M. Shifman, N. G. Uraltsev and A. Vainshtein, *Phys. Rev. D* **51**, 2217 (1995); A. F. Falk and M. Neubert, *Phys. Rev. D* **47**, 1965 (1993); T. Mannel, *Phys. Rev. D* **50**, 428 (1994).
17. M. Neubert, *Phys. Lett. B* **338**, 84 (1994)
18. The updates on the value of $|V_{cb}|$ from $\bar{B} \rightarrow D^* \ell^- \bar{\nu}$ and $\bar{B} \rightarrow D \ell^- \bar{\nu}$ decay are from <http://www.lns.cornell.edu/~lkg/vcb/vcb.html> and <http://www.lns.cornell.edu/~bloom/newaverage.html>.
19. O. Schneider in *Proceedings of the XVIII International Symposium on Lepton-Photon Interactions*, Hamburg, Germany, July 1997.
20. A. Falk, M. Luke, M. Savage, *Phys. Rev. D* **53**, 2491 (1996); A. Falk, M. Luke, M. Savage, *Phys. Rev. D* **53**, 6316 (1996).
21. A. Anastassov *et al.* (CLEO), PA05-079, Contributed to *International Conference on High Energy Physics*, Warsaw, Poland, 1996.
22. M. Neubert, *Phys. Rep.* **245**, 259 (1994).
23. F. E. Close and A. Wambach, *Phys. Lett. B* **348**, 207 (1995).
24. D. Scora and N. Isgur, *Phys. Rev. D* **52**, 2783 (1995).
25. J. D. Richman and P. R. Burchat, *Rev. Mod. Phys.* **67**, 893 (1995).
26. E. M. Aitala *et al.* (E791), Fermilab-Pub-97/267-E
27. C. R. Allton *et al.*, *Phys. Lett. B* **345**, 513 (1995).
28. S. Gusken *et al.*, Julich Report No. HLRZ-94-74 (1995).

29. M. Nieves *et al.*, Southampton U. Report No. SHEP-94-95-09 (1994).
30. A. Abada *et al.*, *Nucl. Phys. B* **416**, 675 (1994).
31. R. Fulton *et al.* (CLEO), *Phys. Rev. Lett.* **64**, 16 (1990); J. Bartelt *et al.* (CLEO), *Phys. Rev. Lett.* **71**, 4111 (1993); H. Albrecht *et al.* (ARGUS), *Phys. Lett. B* **234**, 409 (1990); H. Albrecht *et al.* (ARGUS), *Phys. Lett. B* **255**, 297 (1991).
32. J. R. Patterson in *Proceedings of the 28th International Conference on High Energy Physics*, Warsaw, Poland, July 1994.
33. D. Buskulic *et al.* (ALEPH), PA05-59, *Proceedings of the 28th International Conference on High Energy Physics*, Warsaw, Poland, July 1994.
34. J. Alexander *et al.* (CLEO), *Phys. Rev. Lett.* **77**, 5000 (1996).
35. J. Adler *et al.* (MARKIII), *Phys. Rev. Lett.* **62**, 1821 (1989).
36. F. Butler *et al.* (CLEO), *Phys. Rev. D* **52**, 2656 (1995); J. Bartelt *et al.* (CLEO), *Phys. Lett. B* **405**, 373 (1997).
37. P. L. Frabetti *et al.* (E687), *Phys. Lett. B* **382**, 312 (1996).
38. E. M. Aitala *et al.* (E791), *Phys. Lett. B* **397**, 325 (1997).
39. K. Kodama *et al.* (E653), *Phys. Lett. B* **316**, 455 (1993).
40. P. L. Frabetti *et al.* (E687), Fermilab-Pub-96/388-E.
41. W. Jaus, *Phys. Rev. D* **53**, 1349 (1996).
42. B. Bajc, S. Fajfer, and R. J. Oakes, *Phys. Rev. D* **53**, 4957 (1996).
43. M. Wirbel, B. Stech, and M. Bauer, *Z. Phys. C* **29**, 637 (1985); M. Wirbel, *Nucl. Phys. B(Proc. Suppl)* **13**, 255 (1990).
44. V. Lubicz, G. Martinelli, M. S. McCarthy, and C. T. Sachrajda, *Phys. Lett. B* **274**, 415 (1992).
45. R. Casalbuoni *et al.*, *Phys. Lett. B* **299**, 139 (1993).
46. I. I. Bigi, B. Blok, M. Shifman, and A. Vainshtein, *Phys. Lett. B* **323**, 408 (1994).
47. K. Honscheid, K. R. Schubert, and R. Waldi, *Z. Phys. C* **63**, 117 (1994).
48. E. Bagan, P. Ball, B. Fiol, and P. Gosdzinsky, *Phys. Lett. B* **351**, 546 (1995); E. Bagan, P. Ball, V. M. Braun, and P. Gosdzinsky, *Phys. Lett. B* **342**, 362 (1995); erratum *Phys. Lett. B* **374**, 363 (1996); M. B. Voloshin, *Phys. Rev. D* **51**, 3948 (1995); M. Buchalla, I. Dunietz, and H. Yamamoto, *Phys. Lett. B* **364**, 188 (1995).
49. M. Neubert and C. T. Sachrajda, *Nucl. Phys. B* **483**, 339 (1997).
50. Review of Particle Properties, *Phys. Rev. D* **54**, (1996).
51. I. Dunietz, J. Incandela, F. Snider, and H. Yamamoto, Fermilab-Pub-96/421-R.
52. I. Dunietz, Fermilab-Pub-96-104-T; I Dunietz, J. Incandela, R. Snider, K. Tesima, and I Watanabe, Fermilab-Pub-96/26-T.
53. L. Gibbons *et al.* (CLEO), *Phys. Rev. D* **56**, 3783 (1997).
54. T. Browder and K. Honscheid, *Prog. in Part. and Nucl. Phys.* **35**, 81 (1995).
55. T. Browder in *Proceedings of 7th International Symposium on Heavy Flavor Physics*, Santa Barbara, California, July, 1997.
56. D. Buskulic *et al.* (ALEPH), CERN-PPE/96-117; G. Alexander *et al.* (OPAL), CERN-PPE/96-51; P. Abreu *et al.* (DELPHI), *Z. Phys. C* **59**, 533 (1993); P. Abreu *et al.* (DELPHI), EPS-0557, Contributed to *International Europhysics Conference on High Energy Physics*, Brussels, Belgium, 1995.

57. S. Glenn *et al.* (CLEO), EPS-0383, Contributed to *International Europhysics Conference on High Energy Physics*, Jerusalem, Israel, 1997.
58. P. Abreu *et al.* (DELPHI), LP-304, Contributed to *XVIII International Symposium on Lepton-Photon Interactions*, Hamburg, Germany, July 1997.
59. K. W. Edwards *et al.* (CLEO), EPS-0346, Contributed to *International Europhysics Conference on High Energy Physics*, Jerusalem, Israel, 1997.
60. M. Gronau, O. F. Hernandez, D. London, and J. Rosner, *Phys. Rev. D* **52**, 6356 (1995).
61. R. Fleischer and T. Mannel, LP-021/022, Contributed to *XVIII International Symposium on Lepton-Photon Interactions*, Hamburg, Germany, July 1997.
62. D. Buskulic *et al.* (ALEPH), *Phys. Lett. B* **384**, 471 (1996); W. Adam *et al.* (DELPHI), *Z. Phys. C* **72**, 207 (1996).
63. M. S. Alam *et al.* (CLEO), EPS-0335, Contributed to *International Europhysics Conference on High Energy Physics*, Jerusalem, Israel, 1997.
64. S. Anderson *et al.* (CLEO), EPS-0333, Contributed to *International Europhysics Conference on High Energy Physics*, Jerusalem, Israel, 1997.
65. D. M. Asner *et al.* (CLEO), EPS-0332, Contributed to *International Europhysics Conference on High Energy Physics*, Jerusalem, Israel, 1997.
66. H. Lipkin, *Phys. Lett. B* **254**, 247 (1991).
67. F. Yuan and K-T. Chao, hep-ph/9706294, June, 1997 and references therein; A. Ali and C. Greub, DESY 97-126, July, 1997; H-Y. Cheng and B. Tseng, IP-ASTP-03-97, NTU-TH-97-08, July, 1997; I Halperin and A. Zhitnitsky, hep-ph/9704412, April, 1997; I Halperin and A. Zhitnitsky, hep-ph/9705251, May, 1997; E. V. Shuryak and A. Zhitnitsky, hep-ph/9706316, June, 1997; I. Dunietz, J. Incandela, F. Snider and H. Yamamoto, Fermilab-Pub-96/421-T, December, 1996; A. Datta, X-G. He, and S. Pakvasa, hep-ph/9707259, July, 1997; A. Kagan and A. Petrov, hep-ph/9707354, July, 1997.
68. R. Ammar *et al.* (CLEO), *Phys. Rev. Lett.* **71**, 674 (1993); CLEO CONF 96-05.
69. A. M. Litke in *Proceedings of the 27th International Conference on High Energy Physics*, Glasgow, Scotland, July, 1994.
70. M. S. Alam *et al.* (CLEO), *Phys. Rev. Lett.* **74**, 2885 (1995)
71. P. G. Colrain and M. I. Williams (ALEPH) Contributed to *The XXXIIInd Rencontres de Moriond: Electroweak Interactions and Unified Theories*, Les Arcs, France March, 1997.
72. K. G. Chetyrkin, M. Misiak, and M. Munz, *Phys. Lett. B* **400**, 206 (1997).
73. A. J. Buras, A. Kwiatkowski, and N. Pott, TUM-HEP-287/97.
74. R. Balest *et al.* (CLEO) in *Proceedings of the 27th International Conference on High Energy Physics*, Glasgow, Scotland, August, 1994.
75. A. Ali, C. Greub, and T. Mannel, DESY 93-016; A. Ali and T. Mannel, *Phys. Lett. B* **264**, 447 (1991); Erratum, *Phys. Lett. B* **274**, 526 (1992).
76. F. Abe *et al.* (CDF), *Phys. Rev. Lett.* **76**, 4675 (1996).
77. S. Glenn *et al.* (CLEO), CLNS97/1514, October, 1997.
78. A. Ali, G. Hiller, L. T. Handoko, T. Morozumi, *Phys. Rev. D* **55**, 4105 (1997).

79. D. Buskulic *et al.* (ALEPH), PA10-019, *Proceedings of the 28th International Conference on High Energy Physics*, Warsaw, Poland, July 1994.
80. G. Buchalla and A. Buras, *Nucl. Phys. B* **400**, 225 (1993).
81. F. Abe *et al.* (CDF), *Phys. Rev. Lett.* **76**, 4675 (1996); updated in <http://www-cdf.fnal.gov/physics/new/bottom/cdf3715/cdf3715.html>.
82. E. M. Aitala *et al.* (E791), *Phys. Rev. Lett.* **76**, 364 (1996).
83. P. L. Frabetti *et al.* (E687), *Phys. Lett. B* **398**, 239 (1997).
84. J. L. Hewett, SLAC-Pub-95-6821, April, 1995.
85. E. H. Thorndike in *Proceedings of the 17th International Conference on Physics in Collision*, Bristol, England, July 1997.